

# Estimation of Relative Subsidence of Collapsible Soils Using Electromagnetic Measurements

Henok Hailemariam, Frank Wuttke

**Abstract**—Collapsible soils are weak soils that appear to be stable in their natural state, normally dry condition, but rapidly deform under saturation (wetting), thus generating large and unexpected settlements which often yield disastrous consequences for structures unwittingly built on such deposits. In this study, a prediction model for the relative subsidence of stressed collapsible soils based on dielectric permittivity measurement is presented. Unlike most existing methods for soil subsidence prediction, this model does not require moisture content as an input parameter, thus providing the opportunity to obtain accurate estimation of the relative subsidence of collapsible soils using dielectric measurement only. The prediction model is developed based on an existing relative subsidence prediction model (which is dependent on soil moisture condition) and an advanced theoretical frequency and temperature-dependent electromagnetic mixing equation (which effectively removes the moisture content dependence of the original relative subsidence prediction model). For large scale sub-surface soil exploration purposes, the spatial sub-surface soil dielectric data over wide areas and high depths of weak (collapsible) soil deposits can be obtained using non-destructive high frequency electromagnetic (HF-EM) measurement techniques such as ground penetrating radar (GPR). For laboratory or small scale in-situ measurements, techniques such as an open-ended coaxial line with widely applicable time domain reflectometry (TDR) or vector network analysers (VNAs) are usually employed to obtain the soil dielectric data. By using soil dielectric data obtained from small or large scale non-destructive HF-EM investigations, the new model can effectively predict the relative subsidence of weak soils without the need to extract samples for moisture content measurement. Some of the resulting benefits are the preservation of the undisturbed nature of the soil as well as a reduction in the investigation costs and analysis time in the identification of weak (problematic) soils. The accuracy of prediction of the presented model is assessed by conducting relative subsidence tests on a collapsible soil at various initial soil conditions and a good match between the model prediction and experimental results is obtained.

**Keywords**—Collapsible soil, relative subsidence, dielectric permittivity, moisture content.

## I. INTRODUCTION

**C**OLLAPSIBLE soils, widely regarded as problematic soils, undergo large volume change when wetted with water, which in turn cause damage to the structures built over them. Naturally occurring collapsible soils usually exist at or near dry state as they are primarily found in arid and semi-arid

regions of the world. The focus of this research is on collapsible soils which may exist at different initial moisture conditions (relative subsidence stages) in remolded or in an undisturbed state in nature.

The triggering mechanism for the stressed relative subsidence of collapsible soils at different initial moisture conditions is mainly attributed to the weakening or softening of a portion of the fine-grained fraction of soil (which exists as a bonding material for the larger-grained particles) [1] and also to the loss of soil strength due to a reduction in matric suction [2] during wetting. The microscopic behavior of collapsible soils is governed by the presence of minerals such as tectosilicates, mica, and clay minerals of smectite, chlorite and kaolinite. The volume change and shear strength in terms of the macroscopic behavior of the individual clay platelets are mostly controlled by surface physicochemical forces, rather than gravitational forces [3]. This is attributed to their small size and the diffuse double layer formed around clay platelets. Comprehensive study of the electromagnetic properties of collapsible soils obtained from HF-EM measurement techniques can be used to quantify the relative subsidence of stressed collapsible soils subjected to wetting processes.

HF-EM measurement techniques such as capacitance methods [4], GPR [5] or TDR [6], [7] work on the basis of detecting changes in spatial and temporal variations of the HF-EM properties at or near the subsurface [8]. At lower frequency ranges from 1 MHz to 200 MHz, capacitance methods such as the parallel-plate configuration are commonly used to determine complex permittivity. In the frequency range from 1 MHz to 10 GHz, time or frequency domain reflectometry techniques are usually employed [9], [10]. Using state-of-the-art geophysical non-destructive HF-EM techniques such as GPR, large scale sub-surface soil exploration and identification of weak (collapsible) soil deposits can be performed by transmitting HF-EM pulses (50 MHz to 1 GHz) from a transmitting antenna in to the ground. By recording the travel time of the emitted pulses through a receiving antenna, the dielectric permittivity of the sub-surface can be obtained, and then used to predict the quantity of the expected relative subsidence of the soil deposit.

Howayek et al. [11] and Ayadat and Hanna [12] have provided a comprehensive review of existing methods for the identification of collapsible soils and estimation of their relative subsidence upon wetting. However, majority of the existing models use soil moisture content as a primary input parameter. This has its limitations both in-situ and in laboratory applications in the estimation of relative subsidence as well as monitoring of the subsidence progress, as the user is

Henok Hailemariam is with the Department of Marine and Land Geomechanics and Geotechnics, Kiel University, Ludewig-Meyn-Straße 10, 24118 Kiel, Germany (phone: +49 – (0) 431 – 880 1976; fax: +49 – (0) 431 – 880 4376; e-mail: henok@gpi.uni-kiel.de).

Frank Wuttke is professor and head of the Department of Marine and Land Geomechanics and Geotechnics, Kiel University, Ludewig-Meyn-Straße 10, 24118 Kiel, Germany (e-mail: fw@gpi.uni-kiel.de).

required to use methods of moisture measurement which disturb the soil structure, or to extract samples for moisture content measurement. This procedure is usually a time-consuming and an un-economic practice in the case that the samples have to be obtained from great sub-surface depths.

To address the aforementioned limitations, a new prediction model, developed using the Minkov et al. [13] model and the advanced Lichtenecker and Rother Model (ALRM) [10], for the relative subsidence of stressed collapsible soils based on soil dielectric permittivity is proposed in this study and its accuracy of prediction is validated by performing relative subsidence tests on collapsible soil at different initial conditions. With the new model, soil relative subsidence can be estimated using porosity, specific gravity and soil dielectric permittivity.

## II. THEORETICAL ANALYSIS

### A. Soil Dielectric Behaviour

Porous mineral materials consist mainly of four phases: solid particles (various mineral phases), pore air, pore fluid as well as a solid particle - pore fluid interface. In principle the fractions of these phases vary both in space (due to composition, specific density and surface area) and time (due to changes of water content, porosity, pore water chemistry and temperature). The electromagnetic properties of the solid particles can be assumed frequency independent in the considered temperature-pressure-frequency range. Real relative permittivity  $\epsilon_G$  of inorganic dielectric mineral materials varies from 3 to 15 [14], [15].

The constitutive broadband electromagnetic transfer functions of a soil sample can be defined in terms of complex relative effective permittivity as:

$$\epsilon_{r,eff}^*(\omega, T, p, \dots) = \frac{\epsilon_{eff}^*(\omega, T, p, \dots)}{\epsilon_0} \quad (1)$$

or effective conductivity as:

$$\sigma_{eff}^*(\omega, T, p, \dots) = j\omega\epsilon_{eff}^*(\omega, T, p, \dots) \quad (2)$$

and complex relative effective magnetic permeability as:

$$\mu_{r,eff}^*(\omega, T, p, \dots) = \frac{\mu_{eff}^*(\omega, T, p, \dots)}{\mu_0} \quad (3)$$

with absolute complex permittivity  $\epsilon_{eff}^*(\omega, T, p, \dots)$  or magnetic permeability  $\mu_{eff}^*(\omega, T, p, \dots)$ , imaginary unit  $j = \sqrt{-1}$ , angular frequency  $\omega = 2\pi f$  as well as permittivity  $\epsilon_0$  and magnetic permeability  $\mu_0$  of free space. The transfer functions depend on frequency  $\omega$  as well as on the thermodynamic state parameters such as temperature  $T$ , pressure  $p$ , and water content  $w$  [10]. In this study, the magnetic permeability was not evaluated. In case of the silty clay soils, the assumption is justified that magnetic effects can be neglected and relative magnetic permeability is equal to 1. The complex relative effective permittivity,  $\epsilon_{r,eff}^* = \epsilon'_{r,eff} - j\epsilon''_{r,eff}$ , has two components, where the real component  $\epsilon'_{r,eff}$  reflects the stored

energy in the soil when it is exposed to time harmonic electromagnetic field with angular frequency  $\omega = 2\pi f$  [8]. While the imaginary part,  $\epsilon''_{r,eff} = \epsilon''_d + \sigma_{DC}/(\omega \epsilon_0)$ , characterizes the Ohmic and polarization losses [16]. Here  $\epsilon''_d$  and  $\sigma_{DC}/(\omega \epsilon_0)$  are the dielectric and conductive losses respectively [6], [17]. The permittivity at different GHz frequencies represents the amount of free water in the soil. Furthermore, the complex permittivity at lower frequencies gives information about the absorbed water [18]. Generally, the polarization of the material (in terms of complex effective permittivity) increases monotonically from microwaves to very low frequencies.

### B. Broadband Dielectric Mixture Model

Due to its simple structure, the theoretical mixing rule according to Lichtenecker and Rother 1931 (typically known as Lichtenecker and Rother Model, LRM), (4), is commonly used in soil physics, remote sensing, geophysics and geotechnical applications [19]-[24].

$$\epsilon_{r,eff}^{*a}(\omega, T, p, \dots) = \sum_{k=1}^N V_k \epsilon_{r,k}^{*a}(\omega, T, p, \dots) \quad (4)$$

where  $\epsilon_{r,eff}^*(\omega, T, p, \dots)$  is the relative effective complex dielectric permittivity of the soil,  $V_k$  is the volume fraction with  $\sum_{k=1}^N V_k = 1$ ,  $\epsilon_{r,k}^*(\omega, T, p, \dots)$  is the corresponding frequency-dependent complex relative permittivity of the  $k$ th component and  $a$  is the so-called exponent or constant structure factor. The LRM is typically known as a three phase (free water, solid grains and air) or four phase (bound water, free water, solid grains and air) mixing rule. The parameter  $a$  contains structural information of free and bound water in soil. However the electromagnetic properties of the bound water phase in soils are poorly understood and difficult to quantify [21], [25] and are consequently neglected in practical applications. Zakri et al. [26] studied the theoretical justification of the LRM based on effective medium theory considering the distribution of depolarization factors linked to the structure parameter  $a$ . The LRM is frequently used with  $a = 1/2$ , and is then called the complex refractive index model (CRIM) [27] or generalized refractive mixing dielectric model (GRMDM) [23]. For  $a = 1/3$ , (4) transforms to the Looyenga-Landau-Lifschitz model (LLLM) [28], [29].

The broadband theoretical frequency and temperature-dependent mixing rule suggested by Wagner et al. [10] based on (4), which is called advanced Lichtenecker and Rother Model (ALRM), (5), is used to analyse the complex dielectric permittivity of the collapsible soil in our study.

$$\epsilon_{r,eff}^{*a(\theta,n)}(\omega, T, p, \dots) = \theta \epsilon_w^{*a(\theta,n)}(\omega, T, p, \dots) + (1-n)\epsilon_G^{a(\theta,n)}(\omega, T, p, \dots) + (n-\theta) \quad (5)$$

where  $n$  is the soil porosity,  $\theta$  is the volumetric water content ( $m^3 m^{-3}$ ),  $\epsilon_w^*(\omega, T, p, \dots)$  is the complex permittivity of pore water, structural exponent  $0 \leq a \leq 1$  and  $\epsilon_G$  is the relative real permittivity of the solid grain particles. A structural exponent  $a = 1/2$  (exponent selected according to CRIM, [27]) is used to analyse the complex dielectric permittivity of the studied collapsible soil, due to its comprehensive use of all soil phase

forms and accuracy of prediction [6], [10], [30].

The pore fluid is considered as an aqueous solution, and the temperature, frequency and porosity-dependent relative effective complex dielectric permittivity is obtained according to the modified Debye model [31], [32]:

$$\varepsilon_w^*(\omega, T, p, \dots) - \varepsilon_\infty(T, p, \dots) = \frac{\varepsilon_s(T, p, \dots) - \varepsilon_\infty(T, p, \dots)}{1 + j\omega\tau(T, p, \dots)} - j \frac{\sigma_{DC}(T, p, \dots)}{\omega\varepsilon_0} \quad (6)$$

with the high frequency limit of permittivity  $\varepsilon_\infty(T, p, \dots)$ , static permittivity  $\varepsilon_s(T, p, \dots)$ , relaxation time  $\tau(T, p, \dots)$ , direct current conductivity contribution  $\sigma_{DC}(T, p, \dots)$  and permittivity of free space  $\varepsilon_0$ . Under atmospheric conditions the dielectric relaxation time of water  $\tau(T)$  depends on temperature  $T$  according to the Eyring equation with Gibbs energy or free enthalpy of activation  $\Delta G_w^\#(T) = \Delta H_w^\#(T) - T\Delta S_w^\#(T)$ , activation enthalpy  $\Delta H_w^\#(T)$  and activation entropy  $\Delta S_w^\#(T)$ . The equation suggested by Dobson et al. [22], (7), is used to obtain the relative real permittivity of the solid grain particles of the studied soils. The term  $G_s$  in (7) represents the specific gravity of solid particles.

$$\varepsilon_G(\omega, T, p, \dots) = (1.01 + 0.44G_s)^2 - 0.062 \quad (7)$$

The ALRM is valid for the full range of soil saturation and takes the mineral composition, soil structure and all soil phase forms along with the coupled hydraulic-structure changes during wetting and drying processes into account.

#### C. Development of the New Model for Predicting the Relative Subsidence of Collapsible Soils

The model for predicting relative subsidence of collapsible soils suggested by Minkov et al. [13] has been modified to develop the new prediction model proposed in our study, due to its simplicity and accuracy of prediction. According to Minkov et al. [13], the relative subsidence ( $\Delta h/h_0$ ) at a stress level of 3 kg cm<sup>-2</sup> (300 kPa), also represented as  $\delta_{np,3}$ , of collapsible soils can be obtained by using the relations given by (8) in percentage or (9) in fraction. The level of stress taken for the model (i.e. 300 kPa) is a representative stress state for collapsible soils, as the maximum relative subsidence of most collapsible soils occurs at a stress level ranging between 200 and 400 kPa. Test results analysing the variation of relative subsidence with applied vertical stress for the collapsible soil studied in this research are in agreement with this criteria (see Section IV B).

$$\Delta h/h_0 = K(n_0 - 40)(30 - w_0) \quad (8)$$

$$\Delta h/h_0 = 100K(n_0 - 0.4)(0.3 - w_0) \quad (9)$$

where,  $\Delta h$  is the change in collapsible soil height resulting from wetting,  $h_0$  is the initial height of soil,  $n_0$  is the initial porosity,  $w_0$  is the initial gravimetric water content, and  $K$  is a soil texture constant with values of 0.02, 0.03, 0.05, 0.08 and 0.09 for loessy sand, sandy loess, typical loess, clayey loess and loessy clay, respectively. According to the model, the relative subsidence is always greater than zero, and the soil

initial porosity and initial gravimetric moisture content should be greater than 0.4 and less than 0.3, respectively in order for subsidence to occur. This criterion complies well with other findings such as Feda [33], Jennings and Knight [34] and others, and typifies the fact that collapsible soils are more susceptible to subsidence when they are in loose state and having a low degree of saturation.

The new model for the prediction of relative subsidence based on complex dielectric permittivity measurement is developed by substituting for the moisture content term in the Minkov et al. [13] model with its equivalent in terms of dielectric permittivity from the ALRM.

Equation (5) can be rewritten in terms of the real component of relative effective complex dielectric permittivity of soil  $\varepsilon'_{r,eff}$  and the real component of relative effective complex dielectric permittivity of water  $\varepsilon'_w$  as:

$$\varepsilon'_{r,eff} = \theta_0 \varepsilon_w'^a + (1 - n_0) \varepsilon_G^a + (n_0 - \theta_0) \quad (10)$$

Equation (10) can be rewritten in terms of the initial volumetric water content  $\theta_0$  of soil as:

$$\theta_0 = (\varepsilon'_{r,eff} - (1 - n_0) \varepsilon_G^a - n_0) / (\varepsilon_w'^a - 1) \quad (11)$$

The initial volumetric water content  $\theta_0$  of a soil can also be expressed in terms of initial gravimetric water content  $w_0$  as:

$$\theta_0 = w_0 G_s (1 - n_0) \quad (12)$$

Combining (11) and (12), we get:

$$w_0 = \frac{\varepsilon'_{r,eff} - (1 - n_0) \varepsilon_G^a - n_0}{G_s (\varepsilon_w'^a - 1) (1 - n_0)} \quad (13)$$

The relative subsidence prediction model which is independent of moisture content is thus obtained by substituting for the value of  $w_0$  from (13) in to (9) as:

$$\Delta h/h_0 = 100K(n_0 - 0.4) \left( 0.3 - \frac{\varepsilon'_{r,eff} - (1 - n_0) \varepsilon_G^a - n_0}{G_s (\varepsilon_w'^a - 1) (1 - n_0)} \right) \quad (14)$$

where,  $\Delta h$  and  $h_0$  are the changes in height due to wetting and initial height of collapsible soil, respectively. The model is valid for  $n_0 > 0.4$  (initial void ratio  $e_0 > 0.66$ ) and the boundary conditions for the measured values of real  $\varepsilon'_{r,eff}$  component of relative effective complex dielectric permittivity and relative subsidence  $\Delta h/h_0$  can be obtained as follows:

The values of the minimum  $(\varepsilon'_{r,eff})_{min}$  and maximum  $(\varepsilon'_{r,eff})_{max}$  real components of relative effective complex dielectric permittivity of the collapsible soil correspond to  $(\Delta h/h_0)_{max}$  and  $(\Delta h/h_0)_{min}$  in (14), respectively. The lower boundary i.e.  $(\varepsilon'_{r,eff})_{min}$  corresponding to  $(\Delta h/h_0)_{max}$  is found using  $w_0 = 0$  (dry condition) in (13). The upper boundary i.e.  $(\varepsilon'_{r,eff})_{max}$  corresponding to  $(\Delta h/h_0)_{min}$  is solved by putting the value  $w_0 = n_0 / [G_s(1 - n_0)]$  (saturated condition,  $\theta_0 = n_0$ ) or  $w_0 = 0.3$  in (13), whichever is smaller.

The primary input parameters for the new model are porosity, specific gravity of solids and soil dielectric

permittivity. The model is also sensitive to frequency changes in the complex dielectric permittivity analysis in the form of  $\epsilon'_{r,eff}$ ,  $\epsilon_G$  and  $\epsilon'_w$  in (13) and (14). In this manuscript values at 1 GHz frequency only are considered. At this frequency range, information on the free water in the soil can be obtained and the dispersion and absorption soil processes can be compared directly [21], [25], [35].

The main uncertainties (source of error) in the use of the new model to predict the relative subsidence of collapsible soils from dielectric measurements are related to errors in the measurement of the relative effective complex dielectric permittivity due to a higher grain size (as in soils with a higher coarse-grain fraction) when an open-ended coaxial line technique is used to obtain the complex dielectric permittivity, and errors due to the precision and calibration procedure of the electromagnetic device (GPR, TDR etc), type of coaxial cables, connectors and used inversion algorithms (if any).

For a typical collapsible soil with specific gravity of solid particles  $G_s = 2.74$ ,  $\epsilon_G = (1.01 + 0.44G_s)^2 - 0.062 = 4.847$ ,  $\epsilon'_w @ 1 \text{ GHz} = 80$  and structural exponent  $a = 1/2$ , (13) and (14) can be simplified to (15) and (16), respectively:

$$w_0 = \frac{\epsilon'^{10.5}_{r,eff} + 1.202n_0 - 2.202}{21.767(1-n_0)} \quad (15)$$

$$\Delta h/h_0 = 100K(n_0 - 0.4) \left( 0.3 - \frac{\epsilon'^{10.5}_{r,eff} + 1.202n_0 - 2.202}{21.767(1-n_0)} \right) \quad (16)$$

with  $(\epsilon'_{r,eff})_{min}$  and  $(\epsilon'_{r,eff})_{max}$  obtained from (15) as:

$$(\epsilon'_{r,eff})_{min} = (2.202 - 1.202n_0)^2 \quad (17)$$

$$(\epsilon'_{r,eff})_{max} = (6.742 + 2.202n_0)^2 \text{ or } (8.732 - 7.732n_0)^2, \text{ whichever is smaller} \quad (18)$$

To assess the accuracy of prediction of the new model, the root mean square error (RMSE), normalized root mean square error (NRMSE) and bias in model prediction are calculated as:

$$RMSE = \sqrt{\frac{\sum [(\frac{\Delta h}{h_0})_m - (\frac{\Delta h}{h_0})_p]^2}{m}} \quad (19)$$

$$NRMSE = \frac{RMSE}{[(\frac{\Delta h}{h_0})_{m,max} - (\frac{\Delta h}{h_0})_{m,min}]} \quad (20)$$

$$bias = \frac{\sum [(\frac{\Delta h}{h_0})_m - (\frac{\Delta h}{h_0})_p]}{m} \quad (21)$$

where,  $m$  is the number of measurements,  $(\Delta h/h_0)_m$  &  $(\Delta h/h_0)_p$  are the measured and predicted values of soil relative subsidence at 300 kPa, respectively, and  $(\Delta h/h_0)_{m,max}$  &  $(\Delta h/h_0)_{m,min}$  are the maximum and minimum values of the measured soil relative subsidence at 300 kPa, respectively.

### III. EXPERIMENTAL PROGRAM

#### A. Tested Soil

Remolded collapsible soil taken from near Baku area, Azerbaijan, at a depth range of 2.0 m to 2.5 m was used for the experimental investigation. The common geotechnical and physiochemical properties of the collapsible soil (obtained following ASTM D420–D5876 [36]) are listed in Table I. Phase content was determined quantitatively by combined X-ray diffraction (XRD) and X-ray fluorescence (XRF) analysis.

TABLE I  
GEOTECHNICAL AND PHYSIOCHEMICAL PROPERTIES OF THE STUDIED COLLAPSIBLE SOIL

Properties	Values
Specific gravity ( $\text{g cm}^{-3}$ )	2.735
Initial water content $w$ (%)	9.3
Liquid limit (%)	31.3
Plastic limit (%)	17.0
Plastic index (%)	14.3
Clay % (< 0.002 mm)	34
Silt % (0.002 - 0.063 mm)	51
Sand % (0.063 - 2 mm)	15
Gravel % (> 2 mm)	0
Classification (USCS)*	CL
Organic content (%)	5.811
Lime content (%)	12.944
Tecosilicates (%)	44
Mica (%)	25
Smectite (%)	7
Chlorite (%)	5
Kaolinite (%)	3

\* USCS unified soil classification system.

#### B. Experimental Procedure and Test Setup

This section describes the experimental methodology and devices used to assess the accuracy of prediction of the new model by conducting relative subsidence tests on a collapsible soil at various initial soil conditions.

Results of single oedometer collapse tests [37] conducted on the collapsible soil at natural loose condition with initial void ratio  $e_0 = 0.83$  and an initial gravimetric water content  $w = 0.093 \text{ g g}^{-1}$  (natural condition), by inundating the specimen with distilled water (as per ASTM D 5333 [38] guidelines) at stress levels ranging between 12 kPa and 1200 kPa to identify the severity of soil collapse and to study the variation of the relative subsidence with applied stress are presented first. Moreover, a total of 36 relative subsidence tests on the collapsible soil (natural loose condition  $e_0 = 0.83$ ) stressed at 300 kPa and at different initial moisture conditions (different initial complex dielectric permittivity) were performed to evaluate the accuracy of prediction of the new model presented in this research. The collapsible soil specimens were initially prepared according to the desired initial void ratio and initial moisture condition and the initial complex dielectric permittivity of each collapsible soil specimen was measured after placing it in the relative subsidence test apparatus shown in Fig. 1 (a). Then after the desired subsidence load (300 kPa) was applied and sufficient time was provided until the changes

in soil deformation associated to the applied load of each specimen was insignificant. Finally, each specimen was inundated with distilled-deionized water to initiate the soil subsidence mechanism due to inundation and the total relative subsidence data of each specimen was recorded.

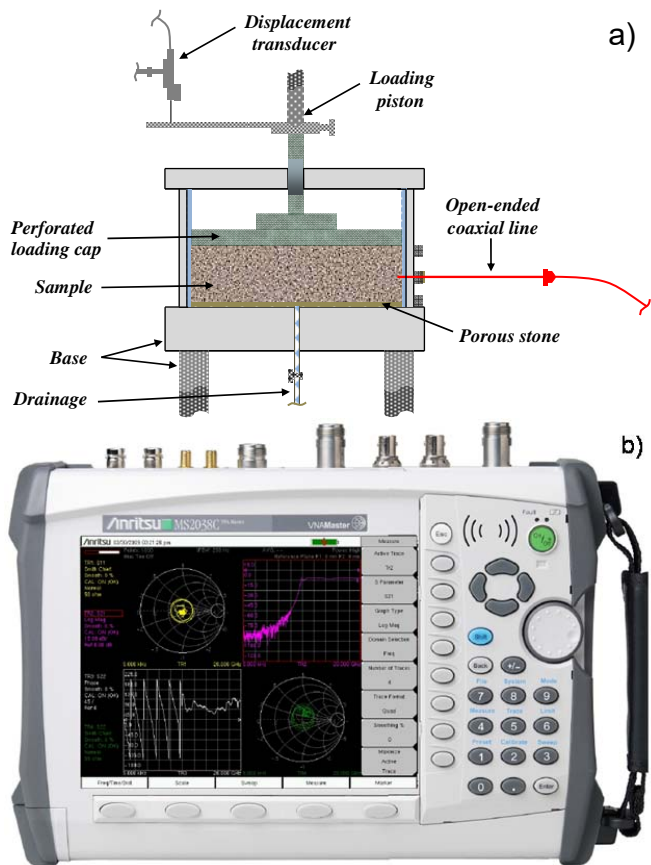


Fig. 1 Experimental setup of the relative subsidence test apparatus (a) and VNA Master MS2027C network analyser (b)

The relative subsidence test apparatus (Fig. 1 (a)) consists of a cylindrical test box, a digital displacement transducer, an open-ended coaxial line, a drainage system for wetting and a controlled loading piston for applying the subsidence load. Electromagnetic measurements were taken with an open-ended coaxial line connected to a VNA Master MS2027C network analyser (Fig. 1 (b)) and fitted horizontally to the test box. The test box consists of an outer steel frame with an inner lining of plexiglass. The outer frame avoids lateral bending that may occur due to loading. The subsidence behavior of collapsible soil depends considerably on the stiffness of the walls of the test box. The use of plexiglass as an inner lining helps to limit the amount of shear stress between the glass wall and the soil mass and ensures that actual plane-strain conditions are met. The digital linear transducer which is attached to the loading piston was used to record the relative subsidence of each specimen during inundation and the data was stored in a data logger connected to the system.

### C. Determination of Soil Complex Dielectric Spectra Using an Open-Ended Coaxial Line Technique

Open-ended coaxial line techniques provide a non-destructive determination of the dielectric spectra of fine-grained soils [39]. The technique was originally developed for the broadband analysis of the dielectric behavior of biological tissues [40], [41], for the microwave dielectric spectroscopy of fluids [42], [43], for food quality determination [44], [45], for geotechnical and physical soil analysis [35], [46] among other applications. The electromagnetic field around the open-ended coaxial probe opening fringes from the interface to the soil specimen and the reflection coefficient measured by means of a HF-EM device can be used to obtain the complex dielectric permittivity of the specimen [40], [47].

The complex impedance  $Z(\omega, T, p, \dots)$  of the sensor-soil-interface depends on the probe geometry and dielectric properties of the soil. The complex impedance  $Z(\omega, T, p, \dots)$  is related to the complex reflection coefficient  $\Gamma(\omega, T, p, \dots)$  as:

$$Z(\omega, T, p, \dots) = Z_0 \frac{[1 - \Gamma(\omega, T, p, \dots)]}{[1 + \Gamma(\omega, T, p, \dots)]} \quad (22)$$

where,  $Z_0$  is the characteristic impedance of the open-ended coaxial probe. It is difficult to obtain the true reflection coefficient  $\Gamma(\omega, T, p, \dots)$  at the aperture plane, due to errors from the connector of the coaxial probe used, type of coaxial line, type of probe head and others. Due to the just mentioned errors, the actual measured reflection coefficient  $S_{11}(\omega, T, p, \dots)$  is not identical with the true reflection coefficient  $\Gamma(\omega, T, p, \dots)$  [40]. To remove these systematic errors, a calibration procedure is normally performed prior to the determination of the soil dielectric spectra [48]. The two commonly used calibration approaches are: i) a two-stage calibration procedure, where in the first stage the  $\Gamma(\omega, T, p, \dots)$  is determined from calibration with three known  $S_{11}(\omega, T, p, \dots)$  reflection coefficients and a second stage where the dielectric permittivity is calculated by means of a theoretical or numerical formulation of the open-ended coaxial system with an infinite ground plane and a semi-infinite sample size [49]-[51], and ii) a single-stage calibration procedure, which is based on a bilinear relationship between  $S_{11}(\omega, T, p, \dots)$  and the complex dielectric permittivities  $\epsilon_{r,eff}^*(\omega, T, p, \dots)$  of reference materials [35], [52], [53].

In this research, the broadband dielectric complex permittivity of the collapsible soil was measured in the frequency range 100 MHz<sup>-1</sup> GHz at room temperature and atmospheric pressure and the calibration procedure based on the second method (i.e. a single-stage bilinear calibration procedure) was adopted to avoid instabilities in the determination of the frequency dependent complex dielectric permittivity due to assumptions in the theoretical formulation of the inverse problem and the numerical implementation of the used open-ended coaxial probe.

Prior to the measurements a full one port three-term calibration was done mechanically at the N (m) connector level of the coaxial cable (N connector is a threaded, weatherproof, medium-size RF connector used to join coaxial

cables) with (Open, Short, 50  $\Omega$ -Match or Load) calibration standards following procedure by Rhode & Schwarz N – 50  $\Omega$  ZV-Z21 to minimize errors in measurement resulting from device. Then after the open-ended coaxial probe (with diameter of 2.2 mm and length of 175 mm) was connected to the calibrated N (m) connector of the coaxial cable and the single-stage bilinear calibration procedure was performed by measuring the complex scattering parameter  $S_{11}(\omega, T, p, \dots)$  of four materials: air, pure methanol, distilled water and a short circuit. The calculation of the relative effective complex dielectric permittivity  $\varepsilon_{r,eff}^*(\omega, T, p, \dots)$  of the soil was obtained as shown in (23) [35].

$$\varepsilon_{r,eff}^*(\omega, T, p, \dots) = \frac{c_1(\omega, T, p, \dots)S_{11}(\omega, T, p, \dots) - c_2(\omega, T, p, \dots)}{c_3(\omega, T, p, \dots) - S_{11}(\omega, T, p, \dots)} \quad (23)$$

where,  $c_i(\omega, T, p, \dots)$  are three frequency, temperature and pressure dependent complex calibration coefficients obtained from the bilinear calibration procedure and  $S_{11}(\omega, T, p, \dots)$  is the measured complex reflection coefficient of the soil specimen. The calibration coefficients are determined with measurements of at least three standard materials with known complex dielectric permittivities in the desired frequency range. The resultant set of equations are assembled in a matrix form as:  $\mathbf{M}(\omega, T, p, \dots) \cdot \mathbf{c}(\omega, T, p, \dots) = \mathbf{e}(\omega, T, p, \dots)$  (see [35]) and are solved for  $\mathbf{c}(\omega, T, p, \dots) = \mathbf{M}^{-1}(\omega, T, p, \dots) \cdot \mathbf{e}(\omega, T, p, \dots)$  numerically using MATLAB. In our study, the three calibration coefficients  $c_i(\omega, T, p, \dots)$  were determined using the so called open-water-liquid (OWL) calibration corresponding to the three standard measurements: air and two well known liquids i.e. distilled water and pure methanol. The temperature of the standard liquids was measured and used to calculate the frequency, temperature and pressure dependent complex dielectric permittivity of water [54] and pure methanol [55] theoretically. Finally a short circuit was measured and used to check the purity of the methanol standard and to improve the accuracy of the calibration in the lower frequency range between 100 MHz to 500 MHz. The relative error of the obtained permittivity depends on the precision of the network analyzer, type of coaxial cables and connectors, used inversion algorithms and other factors. The measured complex dielectric permittivity below 200 MHz is stable and the resultant relative error is lower than 3% [10], [56]. The relative error is of the order of around 5% for frequencies higher than 200 MHz, due to mismatches between connectors, coaxial line and probe.

#### IV. RESULTS AND DISCUSSION

##### A. Calibration Results

In Fig. 2, the real and imaginary parts of the relative effective complex dielectric permittivity  $\varepsilon_{r,eff}^*$  of the calibration standards are shown.

The sensitivity of open-ended coaxial line sensors to determine complex permittivities at lower frequencies around 100 MHz is low (Fig. 2) and the accuracy of the obtained permittivity decreases with dependence on the dynamic range of the instrument, the applied averaging factor (if any), probe

geometry, radiation effects as well as the carefulness of the calibration and measurements. The dielectric spectra (100 MHz to 1 GHz) of the used OWL-Short calibration standards obtained from the VNA measurements are in close agreement with the expected theoretical spectra (Fig. 2). As expected, a good signal-to-noise ratio is recorded for all the calibration standards in the considered frequency range.

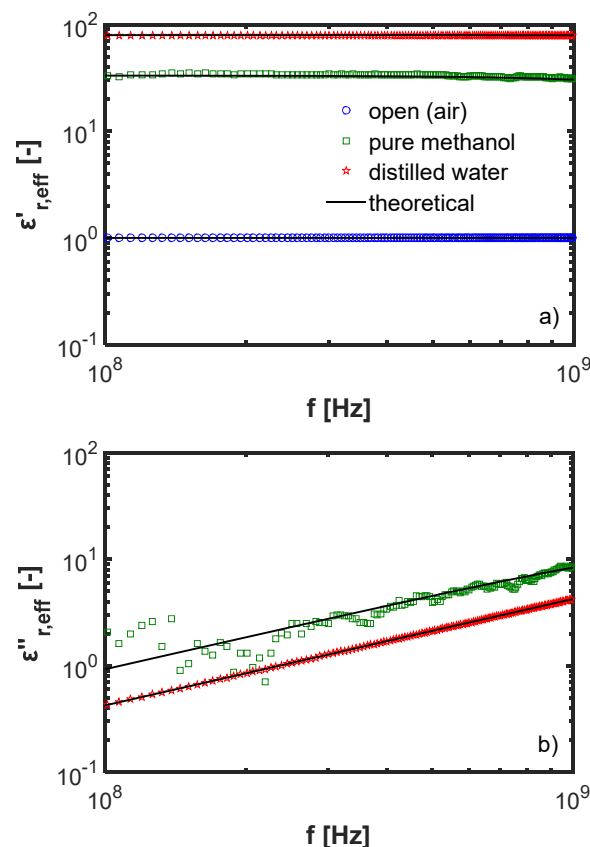


Fig. 2 Obtained dielectric spectra;  $\varepsilon'_{r,eff}$  (a) and  $\varepsilon''_{r,eff}$  (b) with the introduced bilinear calibration procedure (OWL-Short circuit)

##### B. Variation of Relative Subsidence with Stress

Results of single oedometer collapse tests conducted on the collapsible soil initially at natural loose condition  $e_0 = 0.83$  and natural gravimetric water content  $w = 0.093 \text{ g g}^{-1}$  are presented in Fig. 3.

Overall, the relative subsidence of collapsible soils increases with stress. However, the rate of increase of relative subsidence is much higher at lower stress levels and decreases to a minimum at pressures between 200 and 400 kPa. Hence it would be adequate to consider this stress range for analysing the severity of the subsidence potential of collapsible soils. The relative subsidence requires a combination of saturation to dissolve existing bonds and sufficient stress to break the bond between the particles. Hence, when the applied pressure is very low of the order of say 50kPa, it is too small to break the bonds and not large enough to cause a maximal compaction which happens at pressures between 200 and 400kPa. Furthermore, based on the recorded value of relative subsidence of 9.65% at 200 kPa (Fig. 3 (b)), the studied

collapsible soil is classified as soil with severe potential for collapse according to the criteria suggested by Jennings and Knight [34].

previous findings such as Feda [33], Jennings and Knight [34] and others.

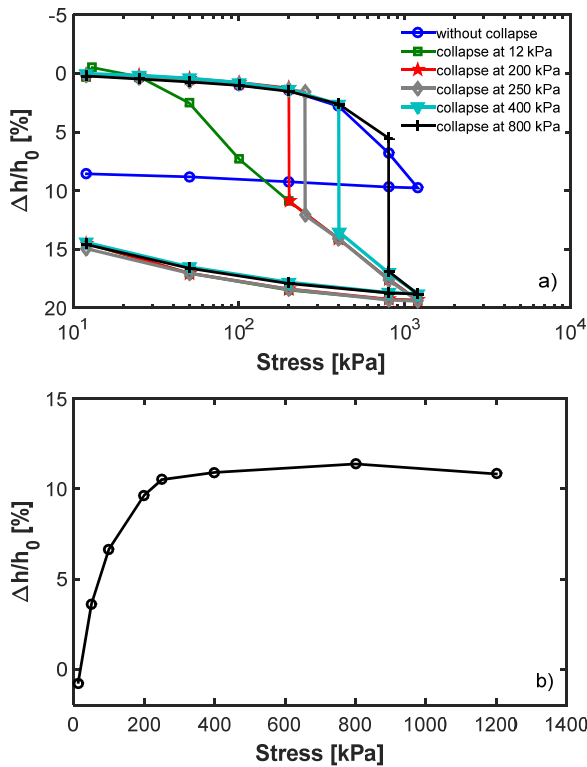


Fig. 3 Single oedometer collapse tests (a) and variation of relative subsidence with stress (b)

### C. New Model Prediction of Relative Subsidence from Dielectric Permittivity

In Fig. 4, model prediction of relative subsidence results obtained using the simplified equation (16) ( $\epsilon_G = 4.847$ ,  $\epsilon'_w @ 1 \text{ GHz} = 80$  and structural exponent  $a = 1/2$ ) for a typical collapsible soil with specific gravity of solid particles  $G_s = 2.74$  are shown.

In Fig. 4 (a), model prediction for five soil texture constants  $K$  of a collapsible soil with porosity  $n = 0.45$  and  $\rho_d = 1.507 \text{ g cm}^{-3}$  (with limits of  $(\epsilon'_{r,eff})_{min} = 2.759$  and  $(\epsilon'_{r,eff})_{max} = 27.415$  obtained using (17) and (18) respectively) is presented. As expected, the soil with the highest soil texture constant  $K=0.09$  (loess clay) exhibits the maximum relative subsidence and vice versa, due to the higher amount of fine-grained fraction (bonding material) present in finer-grained soils as compared with coarser soils, which are then weakened or softened upon wetting resulting in a higher soil subsidence [1], [57]. In Fig. 4 (b), the effect of changes in soil compaction (porosity) on the prediction of relative subsidence of collapsible soils is analysed. For this purpose, model prediction results for five soil porosities of a loessy clay collapsible soil with a soil texture constant  $K=0.09$  are shown. The results are in agreement with the criteria that collapsible soils are more susceptible to subsidence when they are in a loose state and have a low degree of saturation, and complies well with

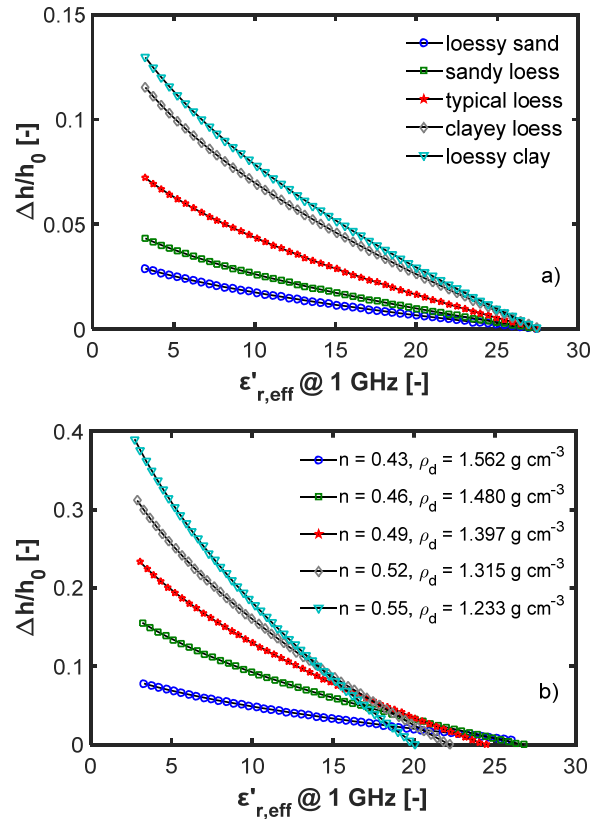


Fig. 4 Variation of  $\Delta h/h_0$  with  $\epsilon'_{r,eff} @ 1 \text{ GHz}$  of a typical collapsible soil for different soil texture (a) and for different values of soil porosity/dry density (b) [results obtained using (16)]

The accuracy of prediction of the new relative subsidence model is evaluated with 36 experimental subsidence tests on the collapsible soil at natural loose condition  $e_0 = 0.83$ , stressed with 300 kPa, and with different initial complex dielectric permittivities, Figs. 5 and 6.

In Fig. 5 (a), plot of the relative subsidence with time of the different specimens recorded immediately after inundation with distilled water is presented. As expected the specimens with a higher measured initial  $\epsilon'_{r,eff} @ 1 \text{ GHz}$  (measured before inundation with distilled water) exhibit a lower relative subsidence and vice versa.

In Figs. 5 (b) and (c), the measured frequency dependence of the relative effective complex dielectric permittivity  $\epsilon^*_{r,eff}$  (dielectric spectra) of the collapsible soil at five soil initial conditions (different moisture contents) is represented. In principle, the open-ended coaxial probe and the calibration procedure used enables an accurate determination of the frequency dependence of the effective complex dielectric permittivity. As expected, apart from the measurements with low complex dielectric permittivity (which corresponds to low soil moisture content) a good signal-to-noise ratio is recorded for all the measurements in the considered frequency range.

In general, clay minerals exhibit high variations of electrical

permittivity with frequency, the phenomenon of which is called dielectric dispersion or relaxation. The magnitude of dielectric dispersion in the frequency range 0.1 MHz-1 GHz is defined as the difference in magnitude at high and low frequencies at which the relative effective complex dielectric permittivity curve levels off. This value has been shown to be highly influenced by the mineralogical and mineral solution interface characteristics of the soil [58]. As expected, a high frequency dependence of  $\epsilon_{r,eff}^*$ , especially at low frequencies [21], is observed for the studied collapsible soil, due to its considerable clay fraction (34 wt.%). Moreover, a strong decrease in the imaginary part  $\epsilon_{r,eff}''$  as compared to the real part  $\epsilon_{r,eff}'$  of the relative effective complex dielectric permittivity with increasing frequency is observed for all cases, mainly due to electrical induced losses.

The plots of model prediction and experimental results of relative subsidence with  $\epsilon_{r,eff}'$  @ 1 GHz, and comparisons between predicted and measured relative subsidence of the collapsible soil are shown in Figs. 6 (a) and (b), respectively. The experimental results match the prediction of relative subsidence of the new model with good accuracy, and values of -0.0003 (-ve = underestimation), 0.0032 and 0.0232 are obtained for the *bias*, *RMSE* and *NRMSE* of relative subsidence model prediction, respectively.

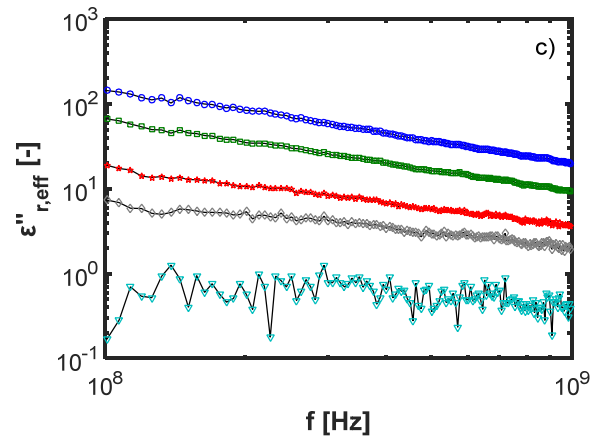
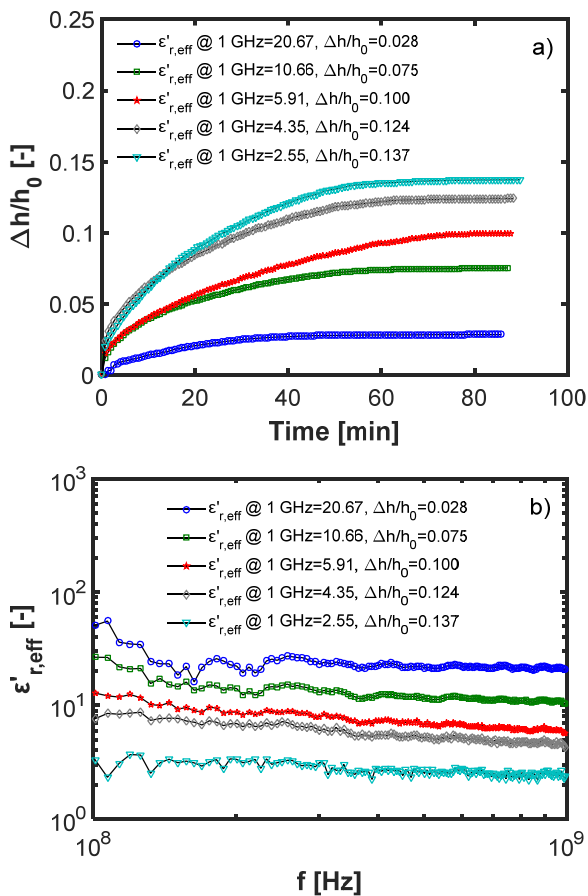


Fig. 5 Plot of the relative subsidence with time of the collapsible soil at different initial conditions (stressed at 300 kPa) (a) and plots of the dielectric spectra for each respective initial condition (b) and (c)

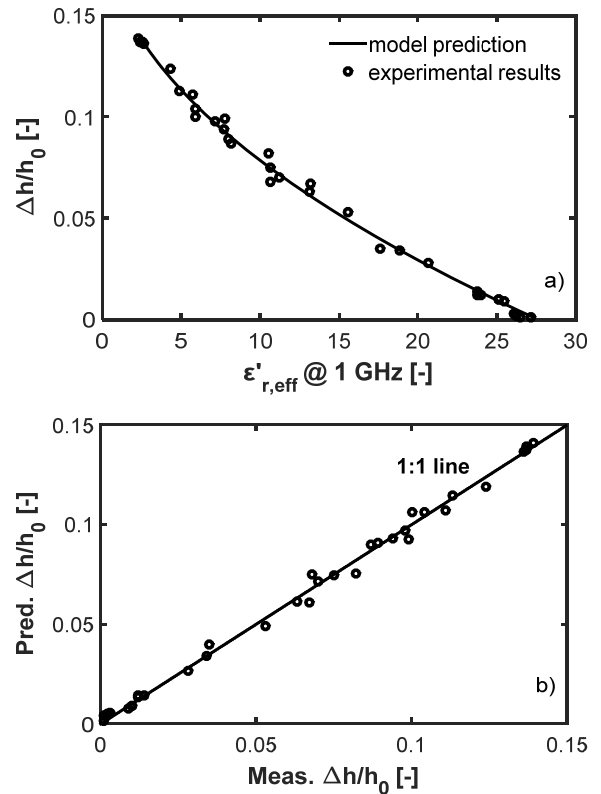


Fig. 6 Comparison between model prediction and experimental results of  $\Delta h/h_0$  with  $\epsilon'_{r,eff}$  @ 1 GHz (a) and predicted vs measured  $\Delta h/h_0$  (b) of the collapsible soil at natural loose condition  $e_0 = 0.83$  and stressed with 300 kPa

## V. CONCLUSIONS

A prediction model for relative subsidence of collapsible soils based on measurements of dielectric permittivity was proposed. With the new model, the relative subsidence of collapsible soils upon wetting can be estimated using porosity, specific gravity of soil solids and real part of the dielectric permittivity. Unlike most relative subsidence prediction

models, the new model does not require moisture content as an input parameter, providing a useful tool in predicting the relative subsidence of weak (collapsible) soil deposits in geotechnical applications, where it is costly (such as in large scale sub-surface analysis of weak deposits) or difficult to obtain soil moisture content data. The accuracy of prediction of the new model was validated by performing subsidence tests on a collapsible soil at various initial conditions with excellent results.

#### ACKNOWLEDGMENT

The authors would like to acknowledge the financial support provided by the German Federal Ministry for Economic Affairs and Energy (BMWi) under Grant number 0325547B and the support of Project Management Jülich.

#### REFERENCES

- [1] A. Casagrande, "The structure of clay and its importance in foundation engineering," *Journal of Boston Society of Civil Engineers*, vol. 19, pp. 168-209, 1932.
- [2] D. G. Fredlund and J. K. M. Gan, "The collapse mechanism of a soil subjected to one-dimensional loading and wetting," Chapter 9: *In Genesis and Properties of Collapsible Soils*, Kluwer Academic Publishers, Boston, NATO ASI Series C: Mathematical and Physical Sciences, vol. 468, pp. 173-205, 1995, [http://dx.doi.org/10.1007/978-94-011-0097-7\\_9](http://dx.doi.org/10.1007/978-94-011-0097-7_9). (Accessed on 11/07/2016)
- [3] B. Lin and A. B. Cerato, "Electromagnetic properties of natural expansive soils under one-dimensional deformation," *Springer-Verlag Berlin Heidelberg*, 2013.
- [4] S. R. Evett, R. C. Schwartz, J. A. Tolk and T. A. Howell, "Soil profile water content determination: spatiotemporal variability of electromagnetic and neutron probe sensors in access tubes," *Vadose Zone Journal*, vol. 8, no. 4, pp. 926-941, 2009, <http://dx.doi.org/10.2136/vzj2008.0146>. (Accessed on 11/07/2016)
- [5] H. M. Jol, "Ground penetrating radar: Theory and applications," *Elsevier*, Amsterdam, Netherlands, 2009.
- [6] D. A. Robinson, S. B. Jones, J. M. Wraith, D. Or and S. P. Friedman, "A review of advances in dielectric and electrical conductivity measurement in soils using time domain reflectometry," *Vadose Zone Journal*, vol. 2, no. 4, pp. 444-475, 2003, <http://dx.doi.org/10.2136/vzj2003.4440>. (Accessed on 11/07/2016)
- [7] D. A. Robinson, C. S. Campbell, J. W. Hopmans, B. K. Hornbuckle, S. B. Jones, R. Knight *et al.*, "Soil moisture measurement for ecological and hydrological watershed-scale observatories: a review," *Vadose Zone Journal*, vol. 7, no. 1, pp. 358-389, 2008, <http://dx.doi.org/10.2136/vzj2007.0143>. (Accessed on 11/07/2016)
- [8] K. Lauer, N. Wagner and P. Felix-Henningsen, "A new technique for measuring broadband dielectric spectra of undisturbed soil samples," *European Journal of Soil Science*, vol. 63, no. 2, pp. 224-238, 2012, <http://dx.doi.org/10.1111/j.1365-2389.2012.01431.x>. (Accessed on 11/07/2016)
- [9] J. Behari, "Microwave dielectric behaviour of wet soils," *Springer*, New York, USA, 2005.
- [10] N. Wagner, K. Emmerich, F. Bonitz and K. Kupfer, "Experimental investigations on the frequency and temperature-dependent dielectric material properties of soil," *IEEE T Geosci Remote*, vol. 49, no. 7, pp. 2518-2530, 2011, <http://dx.doi.org/10.1109/TGRS.2011.2108303>. (Accessed on 11/07/2016)
- [11] A. E. Howayek, P. T. Huang, R. Bisnett and M. C. Santagata, *Identification and behavior of collapsible soils*, Publication FHWA/IN/JTRP-2011/12, Joint Transportation Research Program, Indiana Department of Transportation and Purdue University, West Lafayette, Indiana, USA, 2011, <http://dx.doi.org/10.5703/1288284314625>. (Accessed on 11/07/2016)
- [12] T. Ayadat and A. M. Hanna, "Assessment of soil collapse prediction methods," *IJE Transactions B: Applications*, vol. 25, no. 1, pp. 19-26, 2012, <http://dx.doi.org/10.5829/idosi.ije.2012.25.01b.03>. (Accessed on 11/07/2016)
- [13] M. Minkov, D. Evstatiev, Al. Alexiev and P. Donchev, "Deformation properties of Bulgarian loess soils," in *Proceedings of IX International Conference on Soil Mechanics and Foundation Engineering*, Tokyo, Japan, 1977, pp. 215 - 218.
- [14] J. H. Schoen, *Physical properties of rocks: fundamentals and principles of Petrophysics*. New York: Pergamon, 1996.
- [15] D. A. Robinson and S. P. Friedman, "A method for measuring the solid particle permittivity or electrical conductivity of rocks, sediments, and granular materials," *Journal of Geophysical Research B: Solid Earth*, vol. 108, no. 2, 2003.
- [16] J. B. Hasted, *Aqueous dielectrics*. Chapman and Hall, London, England. 1973.
- [17] G. C. Topp, J. L. Davis and A. P. Annan, "Electromagnetic determination of soil water content: measurements in coaxial transmission lines," *Water Resources Research*, vol. 16, no. 3, pp. 574-582, 1980, <http://dx.doi.org/10.1029/WR016i003p00574>. (Accessed on 11/07/2016)
- [18] J. C. Santamarina and M. Fam, "Changes in dielectric permittivity and shear wave velocity during concentration diffusion," *Canadian Geotechnical Journal*, vol. 32, no. 4, pp. 647-659, 1995, <http://dx.doi.org/10.1139/t95-065>. (Accessed on 11/07/2016)
- [19] K. Lichtenecker and K. Rother, "Die herleitung des logarithmischen mischungsgesetzes aus allgemeinen prinzipien der stationären strömung," *Physikalische Zeitschrift*, vol. 32, pp. 255-260, 1931.
- [20] R. C. Schwartz, S. R. Evett, M. G. Pelletier and J. M. Bell, "Complex permittivity model for time domain reflectometry soil water content sensing: I. Theory," *Soil Science Society of America Journal*, vol. 73, no. 3, pp. 886-897, 2009, <http://dx.doi.org/10.2136/sssaj2008.0194>. (Accessed on 11/07/2016)
- [21] N. Wagner and A. Scheuermann, "On the relationship between matrix potential and dielectric properties of organic free soils: a sensitivity study," *Canadian Geotechnical Journal*, vol. 46, no. 10, pp. 1202-1215, 2009, <http://dx.doi.org/10.1139/T09-055>. (Accessed on 11/07/2016)
- [22] M. C. Dobson, F. T. Ulaby, M. T. Hallikainen and M. A. El-Rayes, "Microwave dielectric behavior of wet soil - Part II: Dielectric mixing models," *IEEE T Geosci Remote*, vol. GE-23, no. 1, pp. 35-46, 1985, <http://dx.doi.org/10.1109/TGRS.1985.289498>. (Accessed on 11/07/2016)
- [23] V. Mironov, M. Dobson, V. Kaupp, S. Komarov and V. Kleshchenko, "Generalized refractive mixing dielectric model for moist soils," *IEEE T Geosci Remote*, vol. 42, no. 4, pp. 773-785, 2004, <http://dx.doi.org/10.1109/TGRS.2003.823288>. (Accessed on 11/07/2016)
- [24] M. Malicki, R. Plagge, M. Renger and R. Walczak, "Application of time domain reflectometry (TDR) soil moisture miniprobe for the determination of unsaturated soil water characteristics from undisturbed soil cores," *Irrigation Science*, vol. 13, no. 2, pp. 65-72, 1992, <http://dx.doi.org/10.1007/BF00193982>. (Accessed on 11/07/2016)
- [25] J. M. Blonquist, S. B. Jr. Jones, I. Lebron and D. A. Robinson, "Microstructural and phase configurational effects determining water content: Dielectric relationships of aggregated porous media," *Water Resources Research*, vol. 42, no. 5, W05424, 2006, <http://dx.doi.org/10.1029/2005WR004418>. (Accessed on 11/07/2016)
- [26] T. Zakri, J. P. Laurent and M. Vauclin, "Theoretical evidence for 'Lichtenecker's mixture formulae' based on the effective medium theory," *Journal of Physics D*, vol. 31, no. 13, pp. 1589-1594, 1998, <http://dx.doi.org/10.1088/0022-3727/31/13/013>. (Accessed on 11/07/2016)
- [27] J. Birchak, C. Gardner, J. Hipp and J. Victor, "High dielectric constant microwave probes for sensing soil moisture," *Proceedings of the IEEE*, vol. 62, no. 1, pp. 93-98, 1974, <http://dx.doi.org/10.1109/PROC.1974.9388>. (Accessed on 11/07/2016)
- [28] L. D. Landau and E. M. Lifshitz, *Elektrodynamik der Kontinua*. AkademieVerlag, Berlin, Germany, 1993.
- [29] J. E. Campbell, "Dielectric properties and influence of conductivity in soils at one to fifty megahertz," *Soil Science Society of America Journal*, vol. 54, no. 2, pp. 332-341, 1990, <http://dx.doi.org/10.2136/sssaj1990.03615995005400020006x>. (Accessed on 11/07/2016)
- [30] J. A. Huisman, S. S. Hubbard, J. D. Redman and A. P. Annan, "Measuring soil water content with ground penetrating radar," *Vadose Zone Journal*, vol. 2, no. 4, pp. 476-491, 2003, <http://dx.doi.org/10.2136/vzj2003.4760>. (Accessed on 11/07/2016)
- [31] U. Kaatze, "Hydrogen network fluctuations and the microwave dielectric properties of liquid water," *Subsurface Sensing Technologies and*

- Applications*, vol. 1, no. 4, pp. 377–391, 2000, <http://dx.doi.org/10.1023/A:1026559430935>. (Accessed on 11/07/2016)
- [32] W. Ellison, “Freshwater and seawater,” in *thermal microwave radiation: Applications for remote sensing*, (Mätzler C (ed.)), The Institution of Engineering and Technology, London, UK, 2006, pp. 431–455.
- [33] J. Fedá, “Structural stability of subsiding loess from Praha-Dejvice,” *Engineering Geology*, vol. 1, pp. 201–219, 1966.
- [34] J. E. Jennings and K. Knight, “A guide to construction on or with materials exhibiting additional settlement due to collapse of grain structure,” in *6<sup>th</sup> Regional Conference for Africa on Soil Mechanics and Foundation Engineering*, Durban, South Africa, September 1975, pp 99–105.
- [35] N. Wagner, M. Schwing and A. Scheuermann, “Numerical 3D FEM and experimental analysis of the open-ended coaxial line technique for microwave dielectric spectroscopy on soil,” *IEEE T Geosci Remote*, vol. 52, no. 2, pp. 880–893, 2014, <http://dx.doi.org/10.1109/TGRS.2013.2245138>. (Accessed on 11/07/2016)
- [36] ASTM, *Annual book of ASTM standards*. Volume 04.08 Soil and Rock (I): D420–D5876 and Volume 4.09 Soil and Rock (II): D5877—latest, American Society for Testing Materials, West Conshohocken, PA, USA, 2011.
- [37] Z. M. Mansour, Z. Chik and M. R. Taha, “On the procedures of soil collapse potential evaluation,” *Journal of Applied Sciences*, vol. 8, no. 23, pp. 4434–4439, 2008, <http://dx.doi.org/10.3923/jas.2008.4434.4439>. (Accessed on 11/07/2016)
- [38] ASTM D 5333-03, *Standard test method for measurement of collapse potential of soils*. Designation D 5333-03, American Society for Testing Materials, West Conshohocken, PA, USA, 2003.
- [39] M. Schwing, A. Scheuermann and N. Wagner, “Experimental investigation of dielectric parameters of soils during shrinkage,” in *Proceedings of the 1st European Conference on Moisture Measurement, Aquametry*, K. Kupfer, Eds. MFPA Weimar, Weimar, Germany, 2010, pp. 511–519.
- [40] M. A. Stuchly, S. S. Stuchly, “Coaxial line reflection methods for measuring dielectric properties of biological substances at radio and microwave frequencies—A review,” *IEEE Trans Instrum Meas IM*, vol. 29, no. 3, pp. 176–183, 1980.
- [41] T. P. Marsland and S. Evans, “Dielectric measurements with an open-ended coaxial probe,” *IEE Proc.*, vol. 134, no. 4, pp. 341–349, 1987.
- [42] Y. -Z. Wei and S. Sridhar, “Radiation-corrected open-ended coax line technique for dielectric measurements of liquids up to 20 GHz,” *IEEE Transactions on Microwave Theory and Techniques*, vol. 39, no. 3, pp. 526–531, 1991.
- [43] A. Kraszewski, M. A. Stuchly and S. S. Stuchly, “ANA Calibration method for measurements of dielectric properties,” *IEEE Trans Instrum Meas IM*, vol. 32, no. 2, pp. 385–387, 1983.
- [44] M. Kent, R. Knöchel. SEQUID, A New Method for the Objective Measurement of the Quality of Seafood, Final Report, Christian-Albrechts-Universität, Kiel, Germany, 2004.
- [45] O. Schimmer, R. Osen, K. Schönfeld and B. Hemmy, “Detection of added water in seafood using a dielectric time domain reflectometer,” in *Proceedings of the 8th International Conference on Electromagnetic Wave Interaction with Water and Moist Substances*, ISEMA, Espoo, Finland, 2009, pp. 350–357.
- [46] Y. Chen and D. Or, “Effects of Maxwell-Wagner polarization on soil complex dielectric permittivity under variable temperature and electrical conductivity,” *Water Resources Research*, vol. 42, no. 6, W06424, 2006.
- [47] M. A. Stuchly, M. M. Brady, S. S. Stuchly and G. Gajda, “Equivalent circuit of an open-ended coaxial line in a lossy dielectric,” *IEEE Trans Instrum Meas IM*, vol. 31, no. 2, pp. 116–119, 1982.
- [48] D. V. Blackham and D. P. Pollard, “An improved technique for permittivity measurements using a coaxial probe,” *IEEE Trans Instrum Meas IM*, vol. 46, no. 5, pp. 1093–1099, 1997.
- [49] N. Sheen and I. Woodhead, “An open-ended coaxial probe for broadband permittivity measurement of agricultural products,” *J. Agric. Eng. Res.*, vol. 74, no. 2, pp. 193–202, 1999.
- [50] D. Popovic, L. McCartney, C. Beasley, M. Lazebnik, M. Okoniewski, S. Hagness and J. Booske, “Precision open-ended coaxial probes for in vivo and ex vivo dielectric spectroscopy of biological tissues at microwave frequencies,” *IEEE Trans. Micro. Theory Tech.*, vol. 53, no. 5, pp. 1713–1721, 2005.
- [51] G. Otto and W. Chew, “Improved calibration of a large open-ended coaxial probe for dielectric measurements,” *IEEE Trans Instrum Meas*, vol. 40, no. 4, pp. 742–746, 1991.
- [52] J.-Z. Bao, C. C. Davis and M. L. Swicord, “Microwave dielectric measurements of erythrocyte suspensions,” *BIOPHYS. J.*, vol. 66, no. 6, pp. 2173–2180, 1994.
- [53] U. Kaatz, “Techniques for measuring the microwave dielectric properties of materials,” *Metrologia*, vol. 47, no. 2, pp. S91–S113, 2010.
- [54] U. Kaatz, “Reference liquids for the calibration of dielectric sensors and measurement instruments,” *Measurement Science and Technology*, vol. 18, no. 4, pp. 967–976, 2007.
- [55] A. P. Gregory and R. N. Clarke. Tables of the complex permittivity of dielectric reference liquids at frequencies up to 5 GHz, Report MAT 23, NPL, 2009.
- [56] N. Wagner, B. Mueller, K. Kupfer, M. Schwing and A. Scheuermann, “Broadband electromagnetic characterization of two-port rod based transmission lines for dielectric spectroscopy of soil,” in *Proceedings of the 1st European Conference on Moisture Measurement, Aquametry*, K. Kupfer, Eds. MFPA Weimar, Weimar, Germany, 2010, pp. 228–237.
- [57] A. Al-Rawas, “State-of-the-art review of collapsible soils,” *Science and Technology*, Sp. Review, pp. 115–135, 2000.
- [58] K. Arulanandan, “Soil structure: In situ properties and behaviour,” Department of Civil and Environmental Engineering, University of California, Davis, CA, USA, 2003.